IMPROVEMENT AND VALIDATION OF THE WALL HEAT TRANSFER PACKAGE OF RELAP5/MOD3.3

Xiaofei Xiong, Jianqiang Shan, and Junli Gou*
School of Nuclear Science and Technology, Xi'an Jiaotong University
No.28, Xianning West Road, Xi'an, Shaanxi Province, China
niangaohx@gmail.com; jqshan@mail.xjtu.edu.cn; junligou@mail.xjtu.edu.cn

ABSTRACT

The process of energy transfer from heat structure to control volume is determined by the wall-to-fluid heat transfer package which is crucial for the safety analysis codes. The current logic for selection of heat transfer modes of RELAP5/MOD3.3 code is too complex and may result in incorrect heat transfer mode judgment, also, the narrow application scope of film boiling heat transfer correlations may result in large errors in film boiling region which is of paramount importance for the predicted peak clad temperatures during hypothetical LB-LOCAs in PWRs. In this study, a new heat transfer package has been developed and incorporated into the RELAP5/MOD3.3 code. Differing from the original package, the modified one consists of twelve heat transfer modes and proposes a new logic for selection of heat transfer modes. For each mode, the models in the existing safety analysis codes and the leading models in literature have been reviewed in order to determine the best model which can easily be applicable to the RELAP5/MOD3.3 code. Particularly, (1) the latest critical heat flux (CHF) and post dryout (PDO) look-up tables proposed by Groeneveld et al. are selected; (2) a new logic for selection of film boiling and transition boiling heat transfer modes is proposed which use minimum film boiling temperature and critical heat flux temperature as distinguished points. The modified code has been validated by comparing the analysis results with available experimental data from tube post dryout experiments and loss-of-fluid test (LOFT) facility. The calculation results showed that the improved package could better predict the experimental phenomena with higher prediction accuracy.

KEYWORDS

RELAP5/MOD3.3, wall heat transfer package, code verification

1. INTRODUCTION

The light water reactor transient analysis code, RELAP5, was developed at the Idaho National Engineering Laboratory (INEL) for the U. S. Nuclear Regulatory Commission (NRC). Code applications include the accident progress analysis, operator guidelines evaluation and licensing audit calculations [1]. The MOD3.3 version of RELAP5 was produced by improving and extending the modeling based on RELAP5/MOD2 in 1985. The mission of the RELAP5/MOD3.3 development program was to develop a code version suitable for the analysis of all transients and postulated accidents in PWR systems. However, G. T. Analytis, one of the developers of RELAP5/MOD3.3, pointed out that the post-CHF heat transfer package had been shown to give unphysical and erroneous predictions [2].

The process of energy transfer from heat structure to control volume is determined by the wall-to-fluid heat transfer package which is crucial for the safety analysis codes. There exists some defects in the wall heat transfer package of RELAP5/MOD3.3. Firstly, the logic for selection of film boiling and transition boiling heat transfer modes mainly depends on empirical wall temperature and heat flux, which is too complex and may result in incorrect heat transfer mode. Secondly, the narrow application scope of film boiling heat transfer correlations may result in large errors in film boiling region which is of paramount importance for the predicted peak clad temperatures during hypothetical LB-LOCAs in PWRs. For these reasons, a new wall-to-fluid heat transfer package has been proposed in this paper. Differing from the original package, the modified one proposes a new logic for selection of heat transfer modes and incorporates the leading models in literature for each mode.

This work is organized as follows. In Section 2, a brief introduction to the modified package will be made and the main contents include heat transfer modes, the logic for selection of heat transfer modes and the heat transfer correlations embedded in the package. In Section 3, the validation of the modified package will be conducted by comparing the analysis results with available experimental data from tube post dryout experiments and LOFT facility. In Section 4, some reasonable conclusions will be drawn according to the current research work.

2. A BRIEF INTRODUCTION TO WALL HEAT TRANSFER PACKAGE

2.1. Heat Transfer Modes

According to the well-known Nukiyama boiling curve [3], the modified package contains twelve heat transfer modes as shown in Table I. Each mode corresponds to an index number, which indicates the heat transfer pattern between the heat structure surface and the fluid. These heat transfer modes are same as RELAP5/MOD3.3 code.

Table I. Heat Transfer Modes of the Heat Transfer Package.

Mode number	Heat transfer phenomena
0	Convection to non-condensable steam-water mixture
1	Convection at supercritical pressure
2	Convection to single-phase liquid
3	Subcooled nucleate boiling
4	Saturated nucleate boiling
5	Subcooled transition boiling
6	Saturated transition boiling
7	Subcooled film boiling
8	Saturated film boiling
9	Convection to single-phase vapor
10	Filmwise condensation
11	Condensation in steam

2.2. The Logic for Selection of Heat Transfer Modes

The logic of selecting heat transfer modes is based on the pressure (P), wall temperature (T_w), vapor saturation temperature based on vapor partial pressure (T_{spp}), vapor saturation temperature based on total pressure (T_{spt}), fluid temperature (T_f), void fraction (α_g) and non-condensable gas quality (X_n). Fig.1 is the heat transfer mode transition map showing the logic built into the modified code to select the appropriate heat transfer mode [4]. The heat transfer coefficients are determined in one of five subroutines: Convection, NucleateBoiling, TransitionBoiling, FilmBoiling and Condensation. The GenerateVapor subroutine is used to calculate the vapor generation rate next to the wall. The main difference between the two logic is the way to judge the nucleate boiling, transition boiling and film boiling. The logic in RELAP5/MOD3.3 mainly depends on empirical wall temperature and heat flux to judge, while the modified logic uses critical heat flux temperature and minimum film boiling temperature as distinguished points.

2.3. Heat Transfer Correlations

The selection of heat transfer correlations directly affects the value of heat transfer coefficients which determines the final value of wall temperature. Due to different application scopes, calculation accuracy and expression forms of the correlations, it is very important to choose appropriate correlations for each heat transfer mode. Some leading models in literatures have been incorporated into the modified code as shown in Table II. In contrast with RELAP5/MOD3.3, the modified program has made an improvement on the calculation of critical heat flux, film boiling, vapor generation rate and the minimum film boiling temperature.

Particularly, the latest PDO look-up table proposed by Groeneveld et al. is selected. The film-boiling look-up table predicts the database for fully developed film-boiling data with an overall rms error in heat transfer coefficient of 10.56% and an average error of 1.71%. In the modified code, the total heat transfer coefficient is obtained from the PDO look-up table. The heat transfer coefficient to the liquid phase is obtained from Bromely correlation and the heat transfer coefficient to the vapor phase is calculated using the total coefficient and the liquid coefficient. This allocation method could bring good predictions in the following experimental verification. Furthermore, the Forslund-Rohsenow correlation is used in the reflood model.

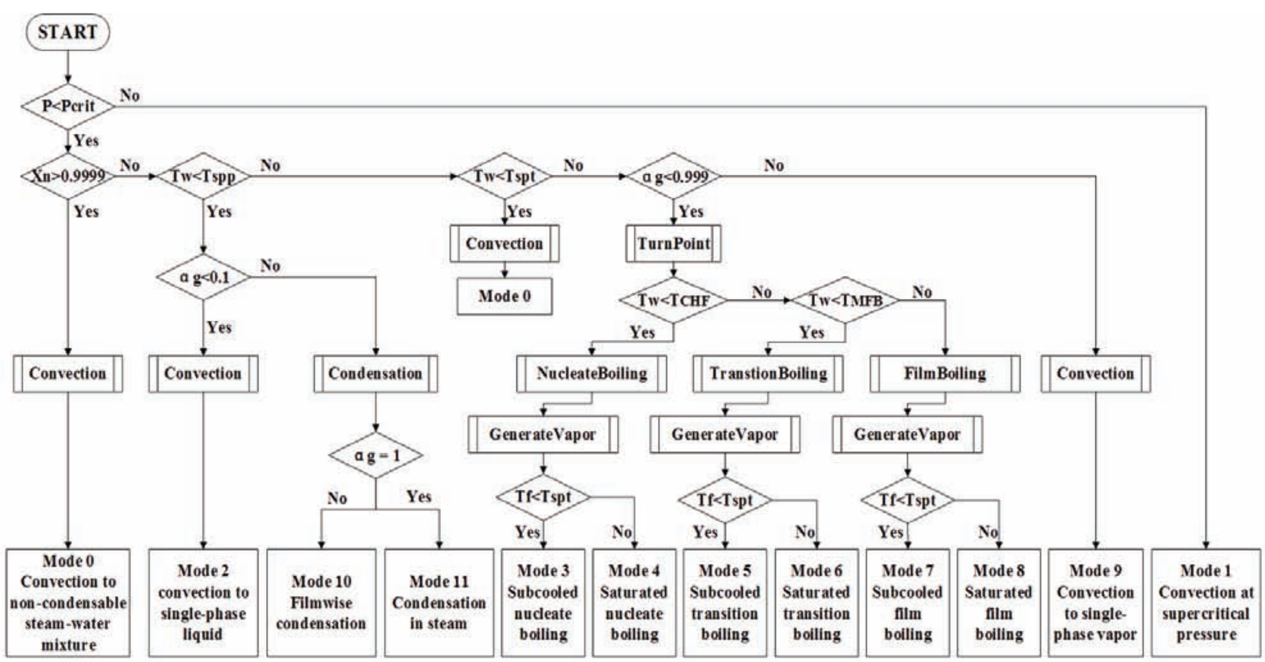

Figure 1. The Modified Logic for Selection of Heat Transfer Modes.

Table II. Heat Transfer Correlations of the Modified Package.

Application	**Correlations**	
Convection	McAdams correlation [5]	$h = 0.59 k_f (\mathrm{Gr} \cdot \mathrm{Pr})^{1/4} / D_h$

Application	Correlations	
	Churchill-Chu correlation [6]	$Nu = \left\{ 0.825 + \frac{0.387(\mathrm{Ra})^{1/6}}{\left[1+\left(\frac{0.492}{\mathrm{Pr}}\right)^{9/16}\right]^{8/27}} \right\}^2$
	Sellar correlation [7]	$h = 4.36k_f / D_h$
	Dittus-Boelter correlation [8]	$h = 0.023 \cdot \mathrm{Re}^{0.8} \cdot \mathrm{Pr}^{0.4}$
Nucleate boiling	Chen correlation [9]	$q'' = h_{mac}(\mathrm{T}_w - T_f)\mathrm{F} + \mathrm{h}_{mic}(\mathrm{T}_w - T_{spt})\mathrm{S}$
Transition boiling	Chen-Sundaram-Ozkaynak correlation [10]	$q_{tb} = q_{CHF} A_f M_f + h_{wgg}(\mathrm{T}_w - \mathrm{T}_g)(1 - \mathrm{A}_f M_f)$ $A_f = e^{-\lambda(\mathrm{T}_w - T_{spt})^{0.5}}$
	Weisman correlation [11]	$h = h_{\max}\left(e^{-0.02\Delta \mathrm{T}_{wchf}}\right) + 4500\left(G / G_R\right)^{0.2}\left(e^{-0.012\Delta \mathrm{T}_{wchf}}\right)$
Film boiling	Groeneveld-Leung PDO look-up table [12]	$h = f(\mathrm{P}, \mathrm{G}, \mathrm{Xe}, \mathrm{T}_w - T_{sat})$
	Forslund-Rohsenow correlation [13]	$h = hl\left\{(g\rho_g\rho_f h_{fg}k^3) / [(\mathrm{T}_w - T_{spt})\mu_g d(\frac{\pi}{6})^{\frac{1}{3}}]\right\}^{0.25}$
	Bromely correlation [14]	$h = 0.62[\frac{g\rho_g k_g^2(\rho_f - \rho_g)\mathrm{h}'_{fg} C_{pg}}{L(\mathrm{T}_w - T_{spt})\mathrm{Pr}_g}]^{0.25} M_a$
Condensation	Nusselt correlation [15]	$h = k_f / \left\{0.9086(\mu_f^2 \mathrm{Re}_f)^{\frac{1}{3}} / [g\rho_f\left(\rho_f - \rho_g\right)]^{\frac{1}{3}}\right\}$
	Chato correlation [16]	$h = 0.296\left[\frac{g\rho_f\left(\rho_f - \rho_g\right)h_{fgb}k_f^3}{D_h\mu_f\left(T_{sppb} - T_w\right)}\right]^{\frac{1}{4}}$
	Shah correlation [17]	$h = h_{sf}\left(1 + 3.8 / Z^{0.95}\right)$ $Z = \left(1/X - 1\right)^{0.8}(\mathrm{P}/\mathrm{P}_{crit})^{0.4}$
Critical heat flux	Groeneveld CHF look-up table developed in 2006 [18]	$q_{CHF} = f(\mathrm{P}, \mathrm{G}, \mathrm{Xe})$
Minimum film boiling temperature	Chen Yuzhou correlation [19]	$T_{MFB} = 363.6 + 38.37 \times \ln P + 0.02844 \times P - 3.86 \times 10^6 \times P^2 + a \times (T_w - T_{sat})$ $\mathrm{a} = \begin{cases} 17.1/(3.3 + 0.0013P) & T_w > T_{sat} \\ 0 & T_w \le T_{sat} \end{cases}$
Vapor generation rate	Lahey correlation [20]	$\Gamma_w = \frac{q''_f A_w}{V[\max(\mathrm{h}_{g,sat} - h_f, 10^4\ J/kg)]} Mul$

3. CODE VALIDATION

In this section, the modified code will be validated and verified by comparing with the results obtained by the original version and with available experimental data. First of all, a number of post dryout tube experiments were calculated, and then a simulation of LOFT facility was performed in the event of the LB-LOCA. Through these comparison and analyses, it can be found that the new package has improved the calculation accuracy.

3.1. Post Dryout Tube Experiments

The post dryout experiments conducted by Bailey in 1969 [21] and Subbotin in 1973 [22] were selected to validate the calculation accuracy of the modified package. The RELAP5 model of the experimental facility is shown in Fig.2. The time-dependent volume 110 and the time-dependent junction 120 simulate the inlet. The pipe 125, which simulates the test section, is linked to a heat structure with the convective left boundary condition, adiabatic right boundary condition and internal heat source. The single junction 128 and the time-dependent volume 130 simulate the outlet. By comparing the wall temperature obtained by the codes with the experiment data, we can verify the modified code.

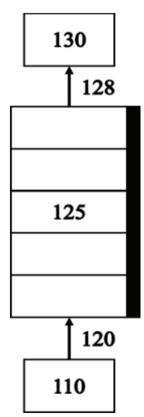

Figure 2. The RELAP5 Model of the experimental Facility.

3.1.1. Validation results of Bailey experiment

Bailey post dryout tube experiment used Winfrith high pressure rig to simulate the phenomenon that the fluid flowed upward in vertical heated tube and exchanged heat with the tube surface, and measured the value of wall temperature under different pressure, mass flow rate, heat flux and inlet sub-cooling conditions. The inner diameter, wall thickness and heated length of the test section are 12.7762 mm, 2.3368 mm and 6.083 m, respectively. The experimental conditions are shown in Table III.

Fig.3 shows the wall temperature versus equilibrium quality of the different cases given in Table III. From the figure, the heat transfer mode changed from nucleate boiling to film boiling along the heated length. The value of wall temperature changed a little during the nucleate boiling, while it increased sharply to a peak value as soon as the mode turned into film boiling.

Table III. Bailey Experimental Conditions.

Experiment number	Pressure (MPa)	Mass flow rate (kg/m^2s)	Average heat flux (W/m^2)	Inlet sub-cooling (kJ/kg)
1490	18.1	4068.7	1078870	131.9
1588	18.0	4095.8	1416411	303.5
1610	17.9	3607.6	1176662	271.4
1616	18.0	3621.1	993696	-81.6
1623	18.0	3621.1	772875	8.6
1634	17.9	2712.5	785493	182.6
1642	17.9	2726.0	463725	-97.9
1650	18.0	2278.5	589908	131.4
1658	17.9	2278.5	362778	-116.1
Range	17.9 ~ 18.1	2278.5 ~ 4095.8	362778 ~ 1416411	-116.1 ~ 303.5

As shown in Fig.3, the modified code and the original one gave the same results of the locations where CHF occurred and the values of CHF were close. Because the new CHF table mainly improved prediction of CHF in the subcooled region and the limiting quality region, in which this experiment didn't involve. The relatively good predicted results by the codes were obtained for most cases, while for 1490 and 1588 cases there were some discrepancies between the predicted results and the experimental data because the CHF look-up table had some error under different pressure, mass flow rate and heat flux conditions. What's more, the improved package better predicted the wall temperatures for all cases. It was chiefly because the new package used the PDO look-up table which was based on a number of experimental data. Compared with the traditional and empirical correlations in MOD3.3, the PDO look-up table has a higher accuracy and a wider range of applications.

3.1.2. Validation results of Subbotin experiment

Similar to Bailey experiment, Subbotin experiment conducted in 1973 also measured the value of wall temperature under different pressure, mass flow rate, heat flux and inlet sub-cooling conditions. The inner diameter of the test section is 10 mm. The experimental conditions are shown in Table IV.

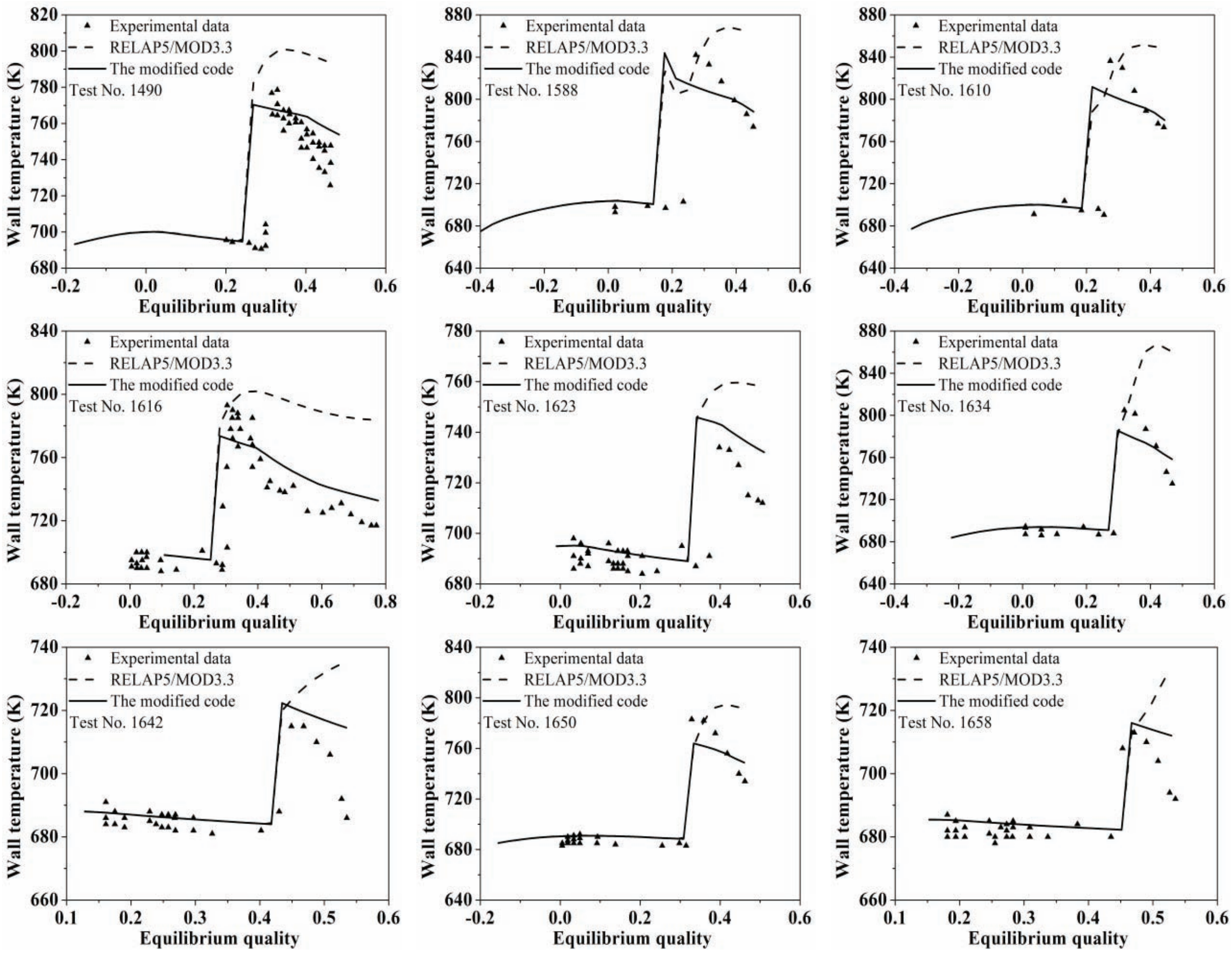

Figure 3. Variation of the Wall Temperature in Bailey Experiment.

Table IV. Subbotin Experimental Conditions.

Experiment number	Pressure (MPa)	Mass flow rate (kg/m^{2}s)	Average heat flux (W/m^2)	Inlet equilibrium quality
1.001	4.9	350	321646	-0.08
1.109	9.8	500	441533	-0.15
1.191	11.8	1000	415638	-0.02
1.274	13.7	1250	510894	-0.09
1.427	17.7	700	365478	-0.3
1.504	19.6	700	430033	-0.75
Range	4.9 ~ 19.6	350 ~ 1250	321646 ~ 611908	-0.75 ~ -0.01

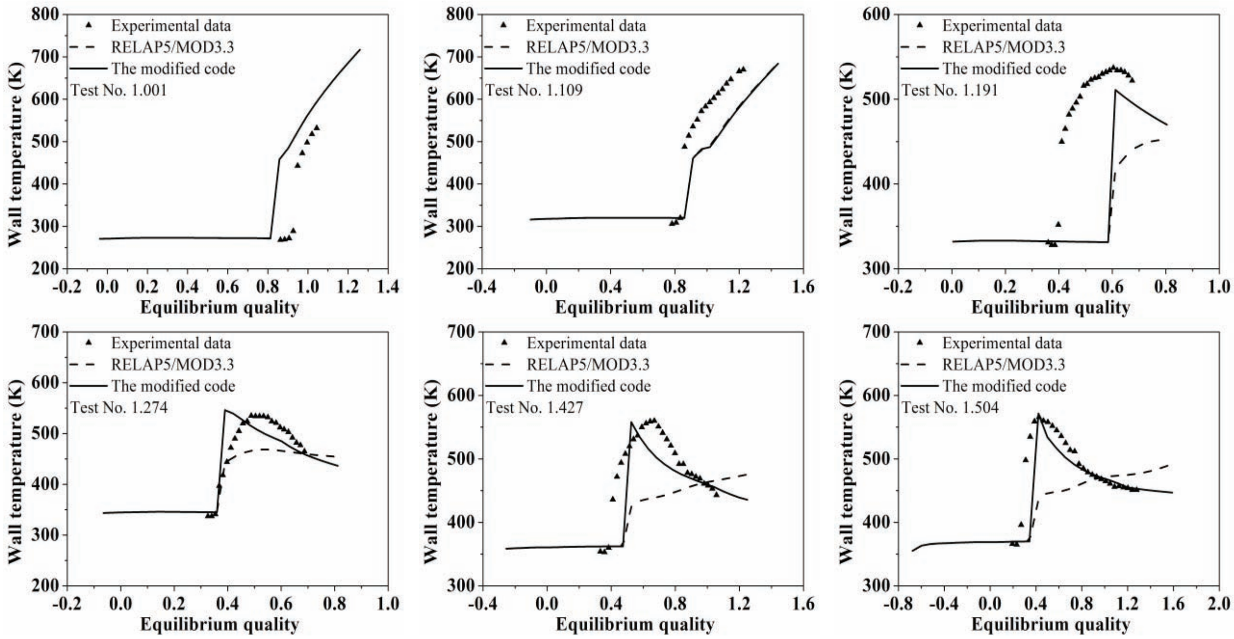

Figure 4. Variation of the Wall Temperature in Subottin Experiment.

The graph of wall temperature versus equilibrium quality is shown in Fig.4. The modified code and the original one gave the same results of locations where CHF occurred under these conditions. Furthermore, the two codes got approximately the same wall temperatures for cases 1.001 and 1.019 because in these conditions, the heat transfer modes changed from the nucleate boiling to the single-phase vapor convection and in this two modes the correlations were approximately same. The result had a big error under 1.191 condition due to the wrong prediction of the location where CHF occurred. For other cases, the improved package better predicted the wall temperature.

3.2. LOFT LB-LOCA Experiment

3.2.1. LOFT experimental facility

The LOFT experimental facility, one of the most prominent reactor safety research facilities in the world, located at the INEL. It was designed on the principle of volume scaling to simulate the major components and system responses of a four-loop commercial PWR during a hypothetical LOCA [23]. The facility consisted of five major systems: the reactor system with the nuclear core, primary coolant system, blowdown suppression system, emergency core cooling system (ECCS) and a secondary coolant system.

The schematic diagram and RELAP5 model of LOFT facility are shown in Fig.5 and Fig.6, respectively. The control volume 230~235 simulate the core, and 220~225 and 240~260 simulate the lower plenum and the upper plenum, respectively. The time-dependent junction 635 and 625 simulate the high pressure safety injection (HPSI) and the low pressure safety injection (LPIS), and the control volume 620 simulates the accumulator. The control volume 415 simulates the pressurizer. The valve 375 is open at steady state and closes once the break happens. The time-dependent volume 700 and 705 simulate the entertainment environment.

3.2.2. Validation results of LOFT LB-LOCA experiment

The initial parameters of LOFT LB-LOCA experiment are close to the condition of operating PWR as shown in Table V. When LOCA occurred at 0s, the core shutdown was triggered by a low pressure signal of pressurizer at 0.13s, and after a delay signal the coolant pump tripped at 0.8s. Then the safety injection system were triggered in sequence. The accumulator opened at 15s, and the HPSI and LPSI began to inject at 22s, 35s, respectively.

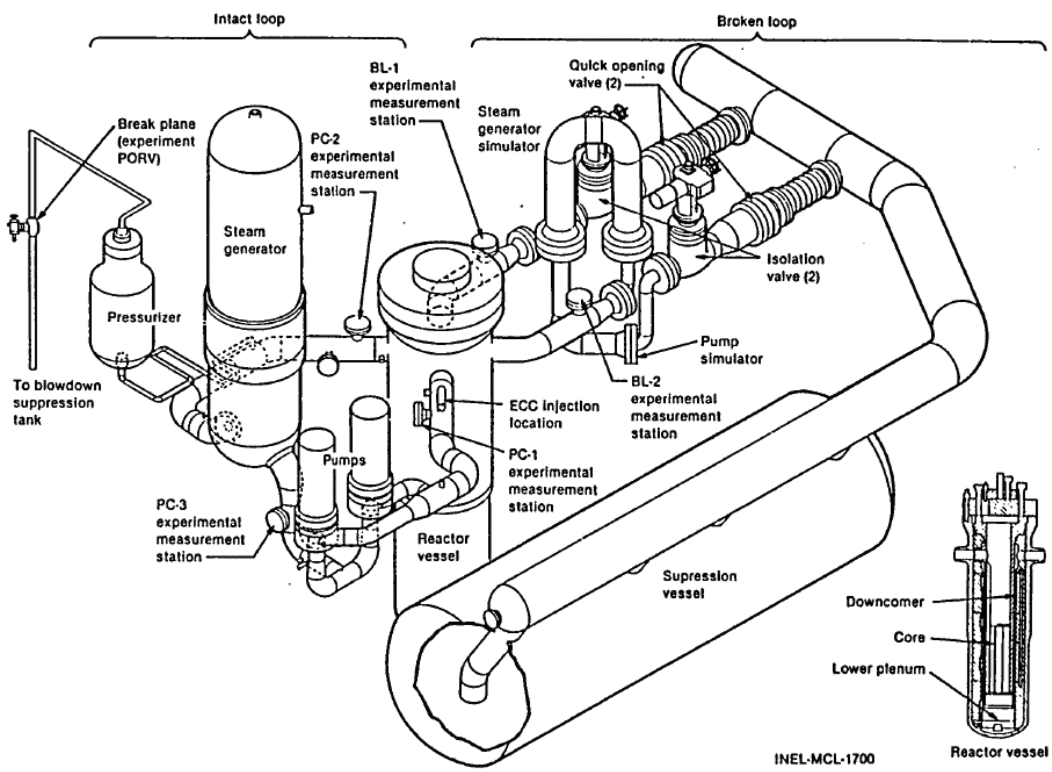

Figure 5. Schematic Diagram of LOFT Facility.

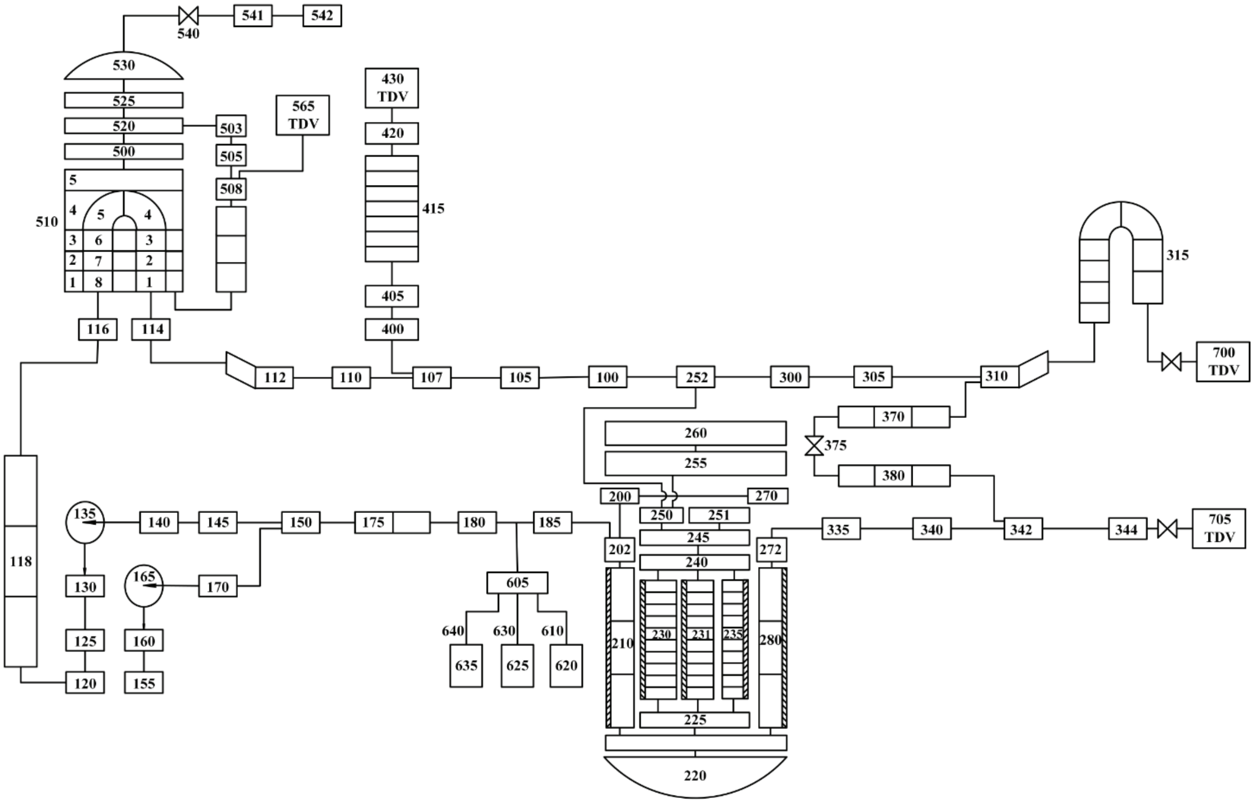

Figure 6. RELAP5 Model of LOFT Facility.

Table V. The Initial Parameters of LOFT LB-LOCA Experiment.

Parameter	Measured value in experiment	Calculated value with code
Core power (MW)	46.0 ± 1.2	46.0
Pressure of the primary loop (MPa)	15.09 ± 0.08	15.10
Cold leg temperature (K)	555.9 ± 1.1	555.99
Hot leg temperature (K)	589.0 ± 1.0	589.1
Mass flow flux of the primary loop (kg/s)	248.7 ± 2.6	248.68
Pressure of the steam generator (MPa)	5.63 ± 0.2	5.63

The variation of main system parameters are shown in Fig.7. When the break occurred at 0s, the pressure of the primary loop dropped rapidly due to the coolant discharge, and then the rate of pressure dropping began to decrease because of coolant boiling which led to a reduction of the break flow rate. The reactor core level decreased after the accident and was almost zero at 3s. Then it recovered slightly because of the coolant pump coasting and the reduction of break flow rate, and the level didn't rise markedly until the LPSI started injecting.

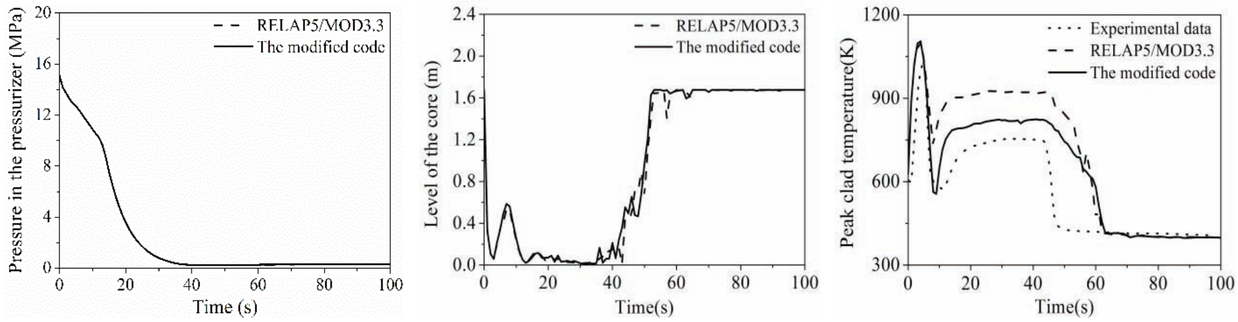

Figure 7. Validation Results of LOFT LB-LOCA Experiment.

As shown in Fig.7, the peak clad temperature rose sharply and reached the peak value quickly after the accident. Afterwards, it dropped by reason of the recovery of core level, and the modified code predicted this phenomenon better. It was mainly because in this rewet period the modified code judged the heat transfer mode as nucleate boiling, while the original code judged it as film boiling which resulted in the higher wall temperature. Then the temperature increased again because the core residual heat couldn't be removed timely and finally it began to decrease continuously due to the action of ECCS. From above, we can see that the improved package better fitted the LOFT experimental data in the prediction of peak clad temperature.

4. CONCLUSIONS

In this work, a modified wall heat transfer package based on RELAP5/MOD3.3 has been developed and verified with available experimental data from tube post dryout experiments and LOFT facility. The conclusions are as follows: (1) by comparing with Bailey and Subbotin tube experiments under various conditions, we found that the modified package could precisely simulate the wall heat transfer phenomenon and had a higher accuracy in the prediction of wall temperature at the post-CHF stage; (2) by comparing with the LOFT LB-LOCA experiment, we saw that the improved package could better predict the pivotal system parameter such as the peak cladding temperature.

ACKNOWLEDGMENTS

The authors appreciate the support from National High-tech Research and Development Program of China (2012AA050905) and the support from China Nuclear Power technology Research Institute (CNPRI).

REFERENCES

1. V. H. Ransom, J. Trapp, and R. Wagner, *RELAP5/MOD3. 3 Code Manual Volume IV: Models and Correlations,* pp. 2, Idaho National Engineering Laboratory, USA (2001).
2. G. T. Analytis, "Study of the Post-CHF Wall Heat Transfer Package of RELAP5/MOD3. 3 During Blow-down," *Annals of Nuclear Energy,* **31**(9), pp. 1053-1068 (2004).
3. S. Nukiyama, "Maximum and Minimum Values of Heat Transmitted from Metal to Boiling Water Under Atmospheric Pressure," *Journal of the Japanese Society of Mechanical Engineers,* **37**, pp. 367 (1934).
4. K. Y. Choi, "Development of a Wall-to-Fluid Heat Transfer Package for the SPACE code," *Nuclear Engineering and Technology,* **41**(9), pp. 1143-1156 (2009).
5. W. H. McAdams, *Heat Transmission, 3rd Edition,* McGraw-Hill, New York, USA (1954).
6. S. W. Churchill and H. H. S. Chu, "Correlating Equations for Laminar and Turbulent Free Convection from a Vertical Plate," *Int. J. Heat Mass Transfer,* **18**, pp. 1323-1329 (1975).
7. J. R. Sellars, M. Tribus, and J. S. Klein, "Heat Transfer to Laminar Flows in a Round Tube or Flat Conduit: The Graetz Problem Extended," *Transaction of the ASME,* **78**, pp. 441 (1956).
8. F. W. Dittus and L. M. K. Boelter, "Heat Transfer in Automobile Radiators of the Tubular Type," *International Communications in Heat and Mass Transfer,* **12**(1), pp. 3-22 (1985).
9. J. C. Chen, "A Correlation for Boiling Heat Transfer to Saturated Fluids in Convective Flow," *Process Design and Development,* **5**, pp. 322-327 (1966).
10. J. C. Chen, R. K. Sundaram, and F. T. Ozkaynak, "A Phenomenological Correlation for Post-CHF Heat Transfer," NUREG-0237(1977).
11. J. Weisman, "Studies of Transition Boiling Heat Transfer at Pressure from 1-4 Bar," EPRINP-1899(1981).
12. D. C. Groeneveld, "A Look-up Table for Fully Developed Film Boiling Heat Transfer," *Nuclear Engineering and Design,* **225**, pp. 83 (2003).
13. R. P. Forslund and W. M. Rohsenow, "Dispersed Flow Film Boiling," *Journal of Heat Transfer,* **90**(4), pp. 399-407(1968).
14. L. A. Bromley, "Heat Transfer in Stable Film Boiling," *Chemical Engineering Progress,* **46**, pp. 221-227 (1950).
15. W. A. Nusselt, "The Surface Condensation of Water Vapor", *Zieschrift Ver. Deut. Ing.* **60**, pp.541 (1916).
16. J. C. Chato, "Laminar Condensation inside Horizontal and Inclined Tubes," *American society of heating, refrigeration and air conditioning engineering journal,* **4**, pp.52 (1962).
17. M. M. Shah, "A General Correlation for Heat Transfer During Film Condensation Inside Pipes," *Int. J. Heat Mass Transfer,* **22**, pp. 547 (1979).
18. D. C. Groeneveld, J. Shan, and A. Z. Vasić, "The 2006 CHF look-up table," *Nuclear Engineering and Design*, **237**(15), pp. 1909-1922 (2007).

19. Y. Chen, "Heat transfer in film boiling of flowing water," *Proceedings of INTECH Theoretical Analysis, Experimental Investigations and Industrial Systems,* pp. 235-260(2011).
20. R. T. Lahey, "A Mechanistic Subcooled Boiling Model," *Proceedings Sixth International Heat Transfer Conference,* Toronto, Canada, August 7-11, 1978, Vol. 1, pp. 293-297(1978).
21. N. A. Bailey and D. H. Lee, *An experimental and analytical study of boiling water at 2000 to 2600 psi,* pp. 2-4, United Kingdom Atomic Energy Authority, UK (1969).
22. V. I. Subbotin, O. V. Remizov, and V. A. Vorobiev, "Temperature Regimes and Heat Transfer in the Region of Degraded Heat Transfer," *IPPE Institute,* **11**, pp. 6-73 (1973).
23. S. M. Modro, et al, "Review of LOFT Large Break Experiments," NUREG0IA-0028 (1989).